Inorganic Chemistry
Article

Inorg. Chem. **2010**, *49*, 7491–7496 **7491**
DOI: 10.1021/ic100790r

Synthesis, Crystal and Electronic Structures, and Physical Properties of Caged Ternary Cu-Rich Antimonide: $BaCu_{7.31(3)}Sb_5$

Wu-Zui Zheng,[†,‡] Peng Wang,[†,‡] Li-Ming Wu,[†] and Ling Chen*[,†]

[†]*Key Laboratory of Optoelectronic Materials Chemistry and Physics, Fujian Institute of Research on the Structure of Matter, Chinese Academy of Sciences, Fuzhou, Fujian 350002, People's Republic of China, and* [‡]*Graduate School of the Chinese Academy of Sciences, Beijing 100039, People's Republic of China*

Received April 23, 2010

A new caged Cu-rich antimonide, $BaCu_{7.31(3)}Sb_5$, was obtained from a direct combination of the elements in a graphite crucible under a high vacuum by a solid state reaction, and the structure was determined by the single-crystal X-ray diffraction method to be hexagonal $P6_3/mmc$ (No.194), with $a = 7.0154(4)$ Å, $c = 12.5423(14)$ Å, $V = 534.58(7)$ Å^3, and $Z = 2$. $BaCu_{7.31(3)}Sb_5$ is the first antimonide member of the $BaNi_9P_5$-type barium copper pnictides with a Cu2 site occupancy of 43.7(9)%, and the structure building unit is a 30-vertex $Cu_{18}Sb_{12}$ cage centered by a Ba atom. The $Cu_{18}Sb_{12}$ cages form chains along the *c* axis by sharing the opposite hexagonal $(Cu2)_3(Sb2)_3$ faces. Such a cage chain shares $(Cu1)_2(Sb1)_2$ rhomboidal faces with six neighboring chains along the [100], [010], and [110] directions to generate a 3D condensed metallic network. The electronic structure calculations by CASTEP indicate the metallic nature, which matches well with the metallic electrical conductivity, small Seebeck coefficient, and Pauli paramagnetism. The calculated formation energies indicate that $BaCu_{7.5}Sb_5 \equiv Ba_2Cu_{15}Sb_{10}$ with the Cu2 site half occupied is the energetically favorable stoichiometry compared with $Ba_2Cu_{12}Sb_{10}$ (empty Cu2 site) and $Ba_2Cu_{18}Sb_{10}$ (fully occupied Cu2 site).

Introduction

Ternary alkaline earth transition metal pnictides have been widely studied for their diverse structural chemistry and potentially interesting properties like thermoelectricity.[1−3] Regarding ternary barium copper pnictides, antimonides are less studied, with only two known examples, BaCuSb[4] and $BaCu_{1.96}Sb_2$,[5] whereas many phosphides and arsenides are reported. For example, BaCuPn is a layered compound and adopts the Ni_2In-type structure.[4,6] $Ba_2Cu_3P_4$ takes a $ThCr_2Si_2$-type layered structure.[7] $BaCu_{1.96}Sb_2$ features parallel chains of 18-vertex cages that share both opposite hexagonal faces and side rhomboidal faces.[5] $Ba_2Cu_{15.33}As_{10}$,[8] an analogue of $BaNi_9P_5$,[9] is a metallic three-dimensional (3D) network, and $BaCu_8Pn_4$ (Pn = P, As),[10] $BaCu_{10}P_4$,[11] and $Ba_8Cu_{16}P_{30}$[12] are all constructed by the primary $CuPn_4$ tetrahedron building unit with a Ba atom locating in either an eight-member ring cavity in $BaCu_8Pn_4$,[10] a heptagonal cavity in $BaCu_{10}P_4$,[11] or a dodecahedron and a tetrakaidecahedron in $Ba_8Cu_{16}P_{30}$.[12]

Here, we report the first copper-rich ternary barium copper antimonide, $BaCu_{7.31(3)}Sb_5$, an analogue of $BaNi_9P_5$-type compounds ($BaNi_9As_5$,[1] $Ba_2Cu_{15.33}As_{10}$,[8] $BaNi_9P_5$,[9] and $SrNi_9P_5$,[13]). Note that the four known $BaNi_9P_5$-type pnictides have shown an inconsistency in the space group. That is, ANi_9Pn_5 (A = Ba, Sr, Pn = P, As) crystallizes in space group $P6_3/mmc$,[1,9,13] while $Ba_2Cu_{15.33}As_{10}$ does so in its subgroup $P\bar{3}1c$.[8] After careful examination, we pointed out that $P6_3/mmc$ should be more reasonable for $BaNi_9P_5$-type compounds, and $Ba_2Cu_{15.33}As_{10}$ should also crystallize in $P6_3/mmc$ instead of its subgroup $P\bar{3}1c$. In addition, the synthesis, crystal structure, electrical conductivity, magnetic susceptibility, and electronic structure are reported.

Experimental Section

Syntheses. The following reactants were stored in an Ar-filled glovebox with controlled oxygen and moisture levels below

*To whom correspondence should be addressed. Tel.: (011)86-591-83704947. E-mail: chenl@fjirsm.ac.cn.

(1) Probst, H.; Mewis, A. *Z. Anorg. Allg. Chem.* **1991**, *597*, 173–182.
(2) Dunner, J.; Mewis, A. *J. Alloys Compd.* **1995**, *221*, 65–69.
(3) Huo, D. X.; Sasakawa, T.; Muro, Y.; Takabatake, T. *Appl. Phys. Lett.* **2003**, *82*, 2640–2642.
(4) Merlo, F.; Pani, M.; Fornasini, M. L. *J Less-Common Met.* **1990**, *166*, 319–327.
(5) Dünner, J.; Mewis, A.; Roepke, M.; Michels, G. *Z. Anorg. Allg. Chem.* **1995**, *621*, 1523–1530.
(6) Mewis, A. *Z. Naturforsch., B* **1979**, *34*, 1373–1376.
(7) Pilchowski, I.; Mewis, A. *Z. Anorg. Allg. Chem.* **1990**, *581*, 173–182.
(8) Kim, S. J.; Ireland, J.; Kannewurf, C. R.; Kanatzidis, M. G. *Chem. Mater.* **2000**, *12*, 3133–3138.
(9) Badding, J. V.; Stacy, A. M. *J. Soild State Chem.* **1990**, *87*, 10–14.
(10) Pilchowski, I.; Mewis, A.; Wenzel, M.; Gruehn, R. *Z. Anorg. Allg. Chem.* **1990**, *588*, 109–116.
(11) Young, D. M.; Charlton, J.; Olmstead, M. M.; Kauzlarich, S. M. *Inorg. Chem.* **1997**, *36*, 2539–2543.
(12) Dünner, J.; Mewis, A. *Z. Anorg. Allg. Chem.* **1995**, *621*, 191–196.
(13) Keimes, V.; Mewis, A. *Z. Kristallogr.* **1993**, *207*, 81–89.

Published on Web 07/22/2010

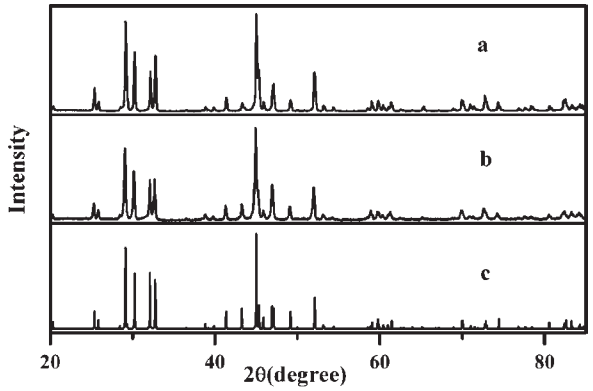

Figure 1. The X-ray powder patterns of (a) the as-synthesized loose gray chunks of $BaCu_{7.31(3)}Sb_5$, (b) the ingot after the electrical conductivity measurement, and (c) the simulated X-ray powder pattern for $BaCu_{7.31(3)}Sb_5$.

0.1 ppm. Ba (rod, 99+%, Alfa Aesar) was filed to remove the oxidized layer before use, and Cu (shot, 99.5%, Alfa Aesar) and Sb (granular, 99.99%, Sinopharm Chemical Reagent Co.,Ltd.) were used as purchased. $BaCu_{7.31(3)}Sb_5$ was initially found as a byproduct in the reactions intending to synthesize $BaCu_{1.96}Sb_2$.[5] The reaction mixture was placed in a graphite crucible and then sealed in an evacuated silica tube under a vacuum at 10^{-3} Pa. The sealed tubes were placed into a temperature-controlled muffle furnace, heated to 950 at 50 °C/h and annealed at that temperature for 80 h, slowly cooled at 3 °C/h to 400 °C, and then cooled from 20 °C/h to room temperature. The resulting block-shaped gray-black crystals were stable in the air over a period of months and were determined to be $BaCu_{7.31(3)}Sb_5$ by single-crystal X-ray diffraction studies.

After the establishment of the structure of $BaCu_{7.31(3)}Sb_5$, a stoichiometric synthesis was carried out and only generated a mixture of the target compound together with a minor byproduct of Cu_2Sb. However, the byproduct Cu_2Sb was irremovable by reannealing the mixture. A series of experiments with Ba/Cu/Sb, 1:*x*:5 (x = 5, 6, 7, 8, 9), indicated that samples obtained from x = 5 and 6 were $BaCu_{7.31(3)}Sb_5$ plus minor Sb and Cu_2Sb, while samples from x = 8 and 9 were a mixture of $BaCu_{7.31(3)}Sb_5$ and Cu_2Sb. Once the Cu amount deviates from 7.3, Cu_2Sb always exits as a byproduct. Finally, we found that Ba had to be loaded in a 5% excess amount with other reactants loaded stoichiometrically. A successful temperature profile entails heating at 12.5 °C/h to 650 °C, annealing for 60 h, slow cooling at 2.5 °C/h to 300 °C, and then radiative cooling to room temperature. The powder X-ray diffraction pattern of the resulting gray loose chunk matches well with that simulated from the single-crystal structure (Figure 1a).

Single-Crystal and Powder X-Ray Diffractions. A gray black bar-shaped crystal ($0.10 \times 0.09 \times 0.08$ mm^3) was mounted on a glass fiber. The single-crystal X-ray diffraction data were collected on a Rigaku Mercury CCD diffractometer equipped with a graphite-monochromated Mo Kα radiation source (λ = 0.71073 Å) at 293 K. The absorption corrections were done using the multiscan method.[14] The observed Laue symmetry and systematic extinctions were indicative of the space group $P6_3/mmc$ (No. 194). The structure was solved by direct methods and refined by full-matrix least-squares fitting on F^2 by SHELXL-97.[15] All of the atoms were refined with anisotropic thermal parameters and a secondary extinction correction. Finally, the atomic positions were standardized with the TIDY program. Crystallographic data and structural refinements are summarized in Table 1. Atomic positions and anisotropic displacement parameters are provided in Table 2. Selected bond lengths are given in Table 3. More details will be presented in the Results and Discussion section below.

(14) *CrystalClear*, version 1.3.5; R. Corp: Woodlands, TX, 1999.
(15) Sheldrick, G. M. *SHELXL-97*; University of Göttingen: Göttingen, Germany, 1997.

Table 1. Selected Data from the Single-Crystal Structure Refinement of $BaCu_{7.31(3)}Sb_5$

empirical formula	$BaCu_{7.31(3)}Sb_5$
fw	1210.57
temp (K)	293(2)
radiation, wavelength (Å)	Mo Kα, λ = 0.71073
cryst syst	hexagonal
space group, Z	$P6_3/mmc$, 2
unit cell dimensions (Å)	a = 7.0154(4)
	c = 12.5423(14)
volume (Å^3)	534.58(7)
calcd density g/cm^3	7.521
absorption coeff (mm^{-1})	30.160
reflns collected/unique	3865/269 [R(int) = 0.0320]
data/restraints/params	269/0/22
GOF on F^2	1.179
final R indices [$I > 2\sigma(I)$][a]	R_1 = 0.0299, wR_2 = 0.0606
largest diff. peak and hole (e/Å^3)	1.785 and −2.829

[a] $R_1 = \sum||F_o| - |F_c||/\sum|F_o|$, $wR_2 = [\sum w(F_o^2 - F_c^2)^2/\sum w(F_o^2)^2]^{1/2}$.

Table 2. Atomic Coordinates, Equivalent Isotropic Displacement Parameters (Å^2) and Site Occupancy for $BaCu_{7.31(3)}Sb_5$

atom	Wyckoff position	x	y	z	U(eq)[a,b]	occupancy
Ba1	2*a*	0	0	0	0.017(1)	1
Cu1	12*k*	0.5422(1)	0.0845(2)	0.1014(1)	0.016(1)	1
Cu2	6*h*	0.2186(4)	0.4372(8)	1/4	0.025(2)	0.437(9)
Sb1	4*f*	1/3	2/3	0.0712(1)	0.011(1)	1
Sb2	6*h*	0.8477(1)	0.6954(2)	1/4	0.034(1)	1

Anisotropic Displacement Parameters (Å$^2 \times 10^3$) for $BaCu_{7.31}Sb_5$[c]

atom	U11	U22	U33	U23	U13	U12
Ba1	20(1)	20(1)	10(1)	0	0	10(1)
Cu1	18(1)	10(1)	17(1)	1(1)	0(1)	5(1)
Cu2	37(3)	15(3)	15(2)	0	0	8(1)
Sb1	11(1)	11(1)	9(1)	0	0	6(1)
Sb2	63(1)	13(1)	7(1)	0	0	6(1)

[a] U(eq) is defined as one-third of the trace of the orthogonalized U_{ij} tensor. [b] See the second part of the table for anisotropic displacement parameters (Å$^2 \times 10^3$) for $BaCu_{7.31}Sb_5$. [c] The anisotropic displacement factor exponent takes the form $-2\pi^2[h^2a^{*2}U_{11} + ... + 2hka^*b^*U_{12}]$.

Powder X-ray diffraction patterns were taken at room temperature on a Rigaku Miniflex Π powder diffractometer, using monochromatized Cu Kα radiation. Data were collected in the range of 2θ = 20 − 85° with scan steps of 0.05°.

Elemental Analyses. Semiquantitative microprobe elemental analysis was performed on a field emission scanning electron microscope (FESEM, JSM6700F) equipped with an energy dispersive X-ray spectroscope (EDX, Oxford INCA). On the crystal of $BaCu_{7.31(3)}Sb_5$ used for single-crystal X-ray diffraction data collection, the EDX results indicated the presence of the elements Ba, Cu, and Sb, and no other element such as C was detected in any case. The EDX analyses gave an average atomic composition of (atomic %) 7.5(2)% Ba, 53.6(28)% Cu, and 38.9(28)% Sb that generates Ba/Cu/Sb = 1:7.15:5.19, which is in good agreement with the composition obtained from the single crystal refinement, $BaCu_{7.31(3)}Sb_5$.

Meanwhile, an Ultima-2 inductively coupled plasma emission spectrometer (ICP-OES) was used to quantitatively determine the composition of the polycrystalline powder of the title compound. The ICP atomic composition results (atomic %) of 7.7(2)% Ba, 54.3(13)% Cu, and 38.1(9)% Sb, i.e., Ba/Cu/Sb = 1:7.08:4.97, agree well with the single crystal refinement, $BaCu_{7.31(3)}Sb_5$.

Table 3. Selected Bond Lengths [Å] for $BaCu_{7.31(3)}Sb_5$

bond	dist.	bond	dist.
Ba1−Sb2 (×6)	3.6409(7)	Ba1−Cu2 (×6)	4.1094
Ba1−Cu1 (×12)	3.7661(5)	Ba1−Sb1 (×6)	4.1479
Cu1−Sb1	2.5663(14)	Cu2−Sb2 (×2)	2.359(4)
Cu1−Cu1 (×2)	2.619(2)	Cu2−Cu2 (×2)	2.415(9)
Cu1−Sb1	2.6405(16)	Cu2−Sb1 (×2)	2.640(3)
Cu1−Sb2 (×2)	2.6972(12)	Cu2−Cu1 (×4)	2.8851(12)
Cu1−Cu1	2.742(3)	Sb1−Cu1 (×3)	2.5663(14)
Cu1−Cu2 (×2)	2.8851(12)	Sb1−Cu2 (×3)	2.640(3)
Sb2−Sb2 (×2)	3.205(2)	Sb1−Cu1 (×3)	2.6405(16)
Sb2−Cu1 (×4)	2.6972(12)	Sb2−Cu2 (×2)	2.359(4)

Physical Property Measurements. The electrical conductivity of the polycrystalline pellet of $BaCu_{7.31(3)}Sb_5$ was measured on the ULVAC ZEM-3 instrument from room-temperature to 180 °C. A pellet with dimensions of about 10 × 3 × 1.6 mm^3 was obtained from the thoroughly ground polycrystalline powder by cold pressing. The pellet achieves a density of ∼74% of the theoretical value. After the electrical conductivity measurement, the XRD analyses show no phase change except several minor peak intensity variations probably arising from the crystal orientation (Figure 1b).

The magnetic susceptibility measurement was performed on a Quantum Design MPMS-XL magnetometer in the temperature range of 2−300 K. The X-ray pure polycrystalline powder was thoroughly ground to minimize the possible anisotropic effects and loaded into a gelatin capsule. The data were corrected for the susceptibility of the container and for the diamagnetic contribution from the ion core.

Electronic Structure Calculations. First principle studies of band structures and densities of state (DOS) were performed with the CASTEP code.[16] The Perdew−Burke−Ernzerh (PBE) generalized gradient approximations (GGA)[17] were employed as the exchange-correlation function. Ultrasoft pseudopotentials[18,19] were used to treat the core electrons, in which the valence atomic configurations were $5s^25p^66s^2$, $3d^{10}4s^1$, and $5s^25p^3$ for Ba, Cu, and Sb, respectively. The number of plane waves was determined using a cutoff energy of 290 eV along with a Monkhorst−Pack k-mesh of 4 × 4 × 2. The atomic formation energies of Ba, Cu, and Sb elements (E_{Ba}, E_{Cu}, and E_{Sb}) are also calculated as the energies per atom in the corresponding bulk metals, which are calculated to be E_{Ba} = −699.2956 eV, E_{Cu} = −1346.7318 eV, and E_{Sb} = −151.0872 eV. A similar definition can be found in ref 29.

The calculation model of $Ba_2Cu_{15}Sb_{10}$ per unit cell was built based on the structural parameters of $BaCu_{7.31(3)}Sb_5 \equiv Ba_2Cu_{14.62(6)}Sb_{10}$ single crystal with small modifications that the occupancy of Cu2 site (6*h*) was treated as 50% instead of the refined result 43.7(9) % for simplicity, One Cu2 atom in the top hexagonal face of the $Cu_{18}Sb_{12}$ cage (Figure 3a) was removed, and two Cu2 atoms in the bottom hexagonal face were removed, thus the symmetry was reduced from $P6_3/mmc$ to *Amm*2.

Results and Discussion

Crystal Structure Determination. As discussed above, the single-crystal X-ray diffraction data reveal that $BaCu_{7.31(3)}Sb_5$ crystallizes in the space group $P6_3/mmc$, and the structure has been solved successfully. $BaCu_{7.31(3)}Sb_5$ is isostructural with ANi_9Pn_5 (A = Ba, Sr; Pn = P, As)[1,9,13] and is the first copper-rich antimonide of the barium copper pnictide family. However, the arsenic analogue $Ba_2Cu_{15.33}As_{10}$ was reported to crystallize in a different space group, $P\bar{3}1c$.[8] Hence, a question has been asked of which space group is more reasonable for the title compound and even for ANi_9Pn_5 (A = Ba, Sr, Pn = P, As)[1,9,13] and $Ba_2Cu_{15.33}As_{10}$?[8] As we know, $P\bar{3}1c$ is a subgroup of $P6_3/mmc$ without the symmetries of mirror planes and 6-fold rotation and screw axes. The most obvious difference between these two space groups is the different Wyckoff site symmetry of the 12*k* site in $P6_3/mmc$ and the 12*i* site in $P\bar{3}1c$. In the $P6_3/mmc$ space group, the mirror plane perpendicular to [100] at the 12*k* site results in a quantitative relationship between its coordinates of *x* and *y*, i.e., $y = 2x$. But in the $P\bar{3}1c$ space group, the *x* and *y* coordinates on the 12*i* site have no apparent relationship because of the absence of any site symmetry element. For example, the 12*k* site coordinates of both $BaCu_{7.31(3)}Sb_5$ and $BaNi_9P_5$, i.e., (0.5422, 0.0845, 0.1014) and (0.5356, 0.0712, 0.1077), indeed show the apparent quantitative relation of $y = 2x$. Note that in $Ba_2Cu_{15.33}As_{10}$,[8] the 12*i* site coordinates of (0.5374, 0.0749, 0.1065) also show an apparent quantitative relation of $y = 2x$; thus space group $P6_3/mmc$ should be more reasonable than $P\bar{3}1c$ for $Ba_2Cu_{15.33}As_{10}$.

$BaCu_{7.31(3)}Sb_5$ has a primitive cell and a Pearson's symbol of *hP*30. The five crystallographically unique sites in the asymmetric unit were assigned as 1 Ba, 2 Cu, and 2 Sb, respectively, on the basis of the interatomic distance and relative equivalent isotropic displacement parameter. With full occupancy, the Cu2 site exhibits a 5-fold larger atomic displacement parameter, 0.096 $Å^2$, than that of Cu1 (0.018 $Å^2$). Subsequently, the occupancy of the Cu2 site was refined freely, resulting in an occupancy of 43.7(9) %, with a temperature factor of 0.025 $Å^2$, and lower *R* values, R_1 = 0.0299 and wR_2 = 0.0606 (Table 1). Such a partial occupancy on the Cu site is a common occurrence in the related Cu-containing compounds. For example, in $Ba_{6.76}Cu_{2.42}Te_{14}$, the occupancies of Cu1 (6*g*) and Cu2 sites (12*k*) were 0.617(8) and 0.095(7), respectively.[20] Similarly, in the As analogue $Ba_2Cu_{15.33}As_{10}$, the occupancy of the Cu2 site was 0.557(8).[8] Our quantitative ICP mass composition results described above supported such a Cu deficiency. We also note that the atomic displacement parameter of Sb2 (0.033 $Å^2$) was 3-fold larger than that of Sb1 (0.011 $Å^2$). So the occupancy of Sb2 was also allowed to vary and converged at 102.06%, revealing a full occupancy within the standard deviation. Splitting Sb2 (6*h* site) to a pair of 12*j* sites, or a combination of 6*h* + 12*j*, both with a SUMP constraint, cannot be converged. Considering that the Sb2 atom is the nearest atom to the Cu2 atom (Sb2−Cu2 = 2.359(4) Å), and Sb2 and Cu2 together define the Cu_3Sb_3 six-member ring on the 30-vertex $Cu_{18}Sb_{12}$ cage as described below, the large displacement parameter of Sb2 may be attributed to the perturbation caused by the partial occupancy of the Cu2 site. In addition, to lower the symmetry to $P\bar{3}1c$ does not change the prolate displacement ellipsoid around Sb2 noticeably either. These results agree with those found on the As2 site in $Ba_2Cu_{15.33}As_{10}$

(16) Segall, M. D.; Lindan, P. J. D.; Probert, M. J.; Pickard, C. J.; Hasnip, P. J.; Clark, S. J.; Payne, M. C. *J. Phys.: Condens. Mater.* **2002**, *14*, 2717–2744.

(17) Perdew, J. P.; Burke, K.; Ernzerhof, M. *Phys. Rev. Lett.* **1996**, *77*, 3865–3868.

(18) Lin, J. S.; Qteish, A.; Payne, M. C.; Heine, V. *Phys. Rev. B* **1993**, *47*, 4174–4180.

(19) Hamann, D. R.; Schluter, M.; Cjiang, C. *Phys. Rev. Lett.* **1979**, *43*, 1494–1497.

(20) Cui, Y. J.; Assoud, A.; Xu, J. X.; Kleinke, H. *Inorg. Chem.* **2007**, *46*, 1215–1221.

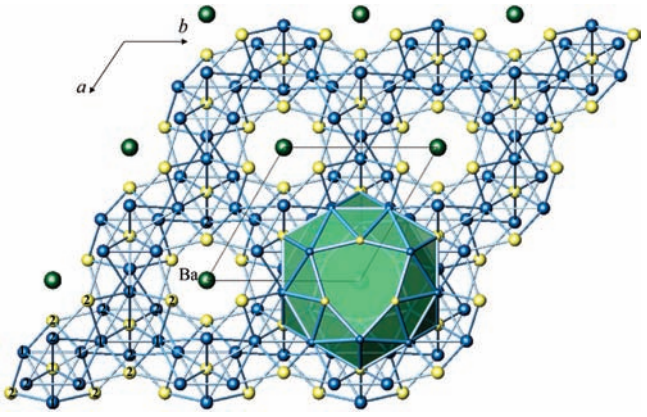

Figure 2. Structure of $BaCu_{7.31(3)}Sb_5$ viewed down the *c* axis with the unit cell outlined and atoms labeled. Ba centers the $Cu_{18}Sb_{12}$ cage (green polyhedron) that forms a chain running along [001] by sharing opposite distorted hexagonal faces. Each cage chain is fused with six neighboring chains along [100], [010], and [110] to generate a 3D condensed network. Green, Ba; blue, Cu; and yellow, Sb. The Cu−Cu and Cu−Sb bonds less than 3.5 Å are drawn.

that was treated as fully occupied in spite of its 5-fold larger displacement parameter (0.032 $Å^2$) in comparison with that of As1 (0.006 $Å^2$).[8]

Structure Description. $BaCu_{7.31(3)}Sb_5$ is isostructural with ANi_9Pn_5 (A = Ba, Sr; Pn = P, As)[1,9,13] with a Cu deficiency on the 6*h* site similar to the arsenic analogue $Ba_2Cu_{15.33}As_{10}$.[8] The 3D condensed anionic framework of $BaCu_{7.31(3)}Sb_5$ is constructed by a 30-vertex cage of $Cu_{18}Sb_{12}$ centered by Ba cation as the building unit (Figure 2). The $Cu_{18}Sb_{12}$ cage (Figure 3a) shares opposite distorted hexagonal faces $(Cu2)_3(Sb2)_3$ to form a chain along the *c* axis (Figure 3b). Each chain shares the side $(Cu1)_2(Sb1)_2$ rhomboidal faces with six neighboring cage chains along the [100], [010], and [110] directions to generate a 3D condensed network (Figures 2, 3).

Ba atom centers the 30-vertex $Cu_{18}Sb_{12}$ cage constructed by 12 Cu1's at a distance of 3.7661(5) Å and six Sb2's at 3.6409(7) Å, together with six Cu2's and six Sb1's at longer distances of 4.1094(35)−4.1479(3) Å (Figure 3a). Such a 30-vertex cage is relatively large among the known caged compounds, for example, the 24-vertex tetrakaidecahedron and 20-vertex dodecahedron in type I clathrate $Ba_8Cu_{16}P_{30}$,[11] the 18-vertex cage in $BaCu_{1.96}Sb_2$,[5] or cages of other clathrates.[21−23]

The local coordination environment of Cu1 (Figure 4a) can be described as a distorted tricapped trigonal prism in which the prism is defined by Cu1 × 2, Cu2 × 2, and Sb1 × 2 with one Cu1 and two Sb2's as the capping atoms. The Cu1−Cu distances vary from 2.619(2) to 2.8851(12) Å, which compares well with the Cu−Cu bond lengths in $BaCu_{10}P_4$ (2.450(2)−3.060(2) Å),[10] the four tetrahedrally bonded Sb atoms generate Cu1−Sb bond lengths in the range of 2.5663(14)−2.697(2) Å, which are comparable to those found in La_6CuSb_{15} (2.498(2)−2.811(2) Å)[24] and $TmCu_{2.935}Sb_2$ (2.553(2)−3.111(2) Å).[25]

The coordination sphere of Cu2 can be described as a distorted bicapped cube in which the cube is defined by two Cu2, two Sb2, and four Cu1 atoms with two Sb1's as capping atoms. The four tetrahedrally arranged Cu2−Sb distances are 2.359(4)−2.640(3) Å, with an average of 2.50 Å, slightly shorter than that of Cu1−Sb (av. 2.65 Å). The average Cu2−Cu length was 2.73 Å, which is similar to the average Cu1−Cu = 2.75 Å. Note that Cu2−Cu2 is 2.415(9) Å, which resembles the Cu2−Cu2 = 2.400(5) in $Ba_2Cu_{15.33}As_{10}$.[8] This Cu2−Cu2 length is about 16% shorter than the Cu2−Cu1 bond, and 9% shorter than the average Cu1−Cu1 bond length; such a shortening may be caused by the positional disorder resulting from the partial occupancy of the Cu2 site.[26]

As shown in Figure 4b, the Sb1 atom is surrounded by nine Cu atoms in a distorted tricapped trigonal antiprismatic geometry with three Cu1's and three Cu2's defining the trigonal bases and three Cu1's as capping atoms. The Sb2 is coordinated by six Cu atoms at 2.359(4)−2.697(2) Å in a very distorted geometry and two Ba atoms at longer distance of 3.6409(7), which is responsible for the distortion around Sb2. The minimum Sb−Sb distance, 3.205(2) Å, is longer than the typical values in Sb_2 pairs (2.8−3.0 Å);[27] thus there is no apparent Sb−Sb bonding interaction in the title compound.

Physical Properties. The temperature dependence of the electrical conductivity and Seebeck coefficient for a $BaCu_{7.31(3)}Sb_5$ polycrystalline pellet with a density of ~74% is shown in Figure 5. The electrical conductivity decreases with increasing temperature, which is in accordance with the metallic behavior. The room-temperature electrical conductivity is about 763 S/cm, comparable to the value of $Yb_{14}MnSb_{11}$ (~500 S/cm at 570K)[28] but lower than the 5882 S/cm measured in the single crystal of the $Ba_2Cu_{15.33}As_{10}$ analogue.[8] The room-temperature Seebeck coefficient (*S*) of $BaCu_{7.31(3)}Sb_5$ is about −3.8 μV/K, and the absolute value shows an increase with the increase of temperature and reaches −5.2 μV/K at 447 K. The absolute values are comparable with the +2.5 μV/K of $Ba_2Cu_{15.33}As_{10}$.[8] The negative sign of *S* means that the majority of carriers in $BaCu_{7.31(3)}Sb_5$ are electrons, indicating metallic behavior.

The magnetic susceptibility of $BaCu_{7.31(3)}Sb_5$ has been measured from 2 to 300 K under an applied field of 1000 Oe. The weak magnetic susceptibility ranges from 8.54×10^{-4} to 1.96×10^{-3} emu/mol and is nearly temperature independent, suggesting Pauli paramagnetism, which agrees with that found in $BaNi_9P_5$.[9] The paramagnetism indicates a metallic behavior, which is consistent with the electrical conductivity.

Electronic Structure. In order to understand the electronic structural characteristics and the related physical properties of $BaCu_{7.31(3)}Sb_5 \equiv Ba_2Cu_{14.62(6)}Sb_{10}$, the densities of state (DOSs) of a model of $Ba_2Cu_{15}Sb_{10}$ with the

(21) Sales, B. C.; Chakoumakos, B. C.; Jin, R.; Thompson, J. R.; Mandrus, D. *Phys. Rev. B* **2001**, *63*(24), 245113.
(22) Nolas, G. S.; Vanderveer, D. G.; Wilkinson, A. P.; Cohn, J. L. *J. Appl. Phys.* **2002**, *91*, 8970–8973.
(23) Bobev, S.; Sevov, S. C. *J. Am. Chem. Soc.* **2001**, *123*, 3389–3390.
(24) Sologub, O.; Vybornov, M.; Rogl, P.; Hiebl, K.; Cordier, G.; Woll, P. *J. Soild State Chem.* **1996**, *122*, 266–272.
(25) Fedyna, L. O.; Bodak, O. I.; Fedorchuk, A. O.; Tokaychuk, Y. O. *J. Alloys Compd.* **2005**, *394*, 156–159.
(26) Xia, S. Q.; Bobev, S. *J. Am. Chem. Soc.* **2007**, *129*, 10011–10018.
(27) Mills, A. M.; Lam, R.; Ferguson, M. J.; Deakin, L.; Mar, A. *Coord. Chem. Rev.* **2002**, *233*, 207–222.
(28) Brown, S. R.; Kauzlarich, S. M.; Gascoin, F.; Synder, G. J. *Chem. Mater.* **2006**, *18*, 1873–1877.
(29) Blake, N. P.; Bryan, D.; Latturner, S.; Mollnitz, L.; Stucky, G. D.; Metiu, H. *J. Chem. Phys.* **2001**, *114*, 10063–10074.

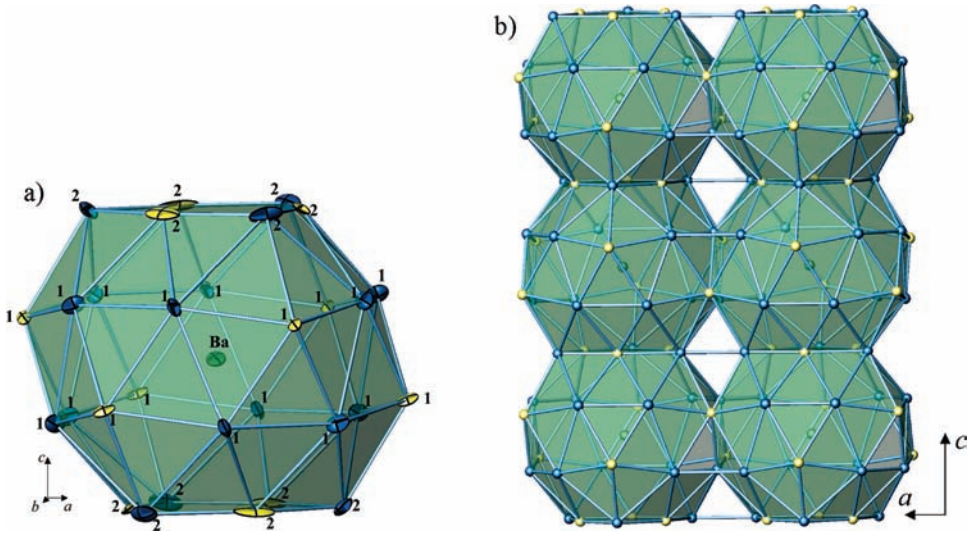

Figure 3. (a) A 30-vertex $Cu_{18}Sb_{12}$ cage in $BaCu_{7.31(3)}Sb_5$ with atoms presented by anisotropic ellipsoids according to their displacement parameters. (b) Two cage chains along the *c* axis are condensed along the *a* direction by fusing the side rhomboidal $(Cu1)_2(Sb1)_2$ faces. Blue, Cu; yellow, Sb. The Cu−Cu and Cu−Sb bonds less than 3.5 Å are drawn.

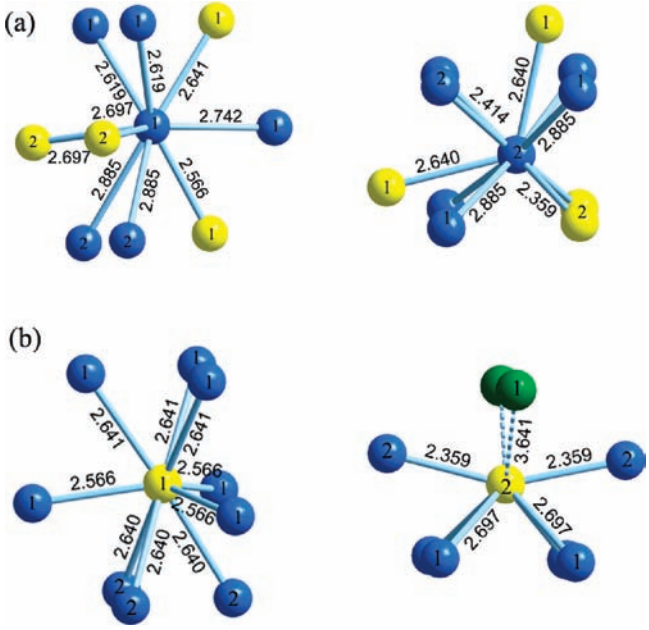

Figure 4. Coordination environments of (a) Cu atoms and (b) Sb atoms in $BaCu_{7.31(3)}Sb_5$ with the bond distances marked. Green, Ba; blue, Cu; yellow, Sb.

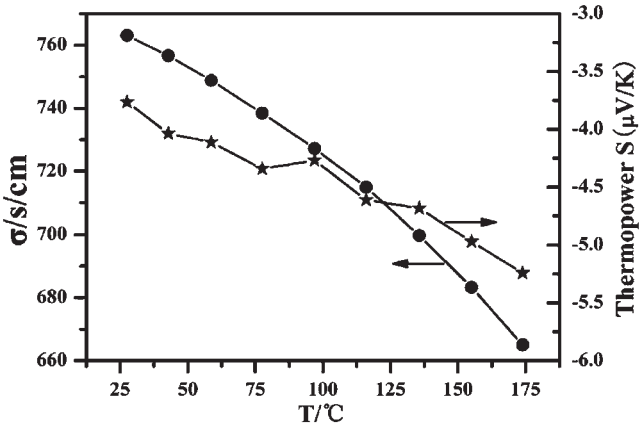

Figure 5. Temperature dependence of the electrical conductivity and Seebeck coefficient for a cold-pressed polycrystalline pellet of $BaCu_{7.31(3)}Sb_5$.

Cu2 site half occupied were calculated. Figure 6 shows that the Fermi level cuts through the DOS curve, indicating a metallic behavior, which matches with the electrical conductivity and Pauli paramagnetic measurements. Below the Fermi level, down to −12 eV, the bands are dominated by Cu 3d and Sb 5p with minor contributions from Cu 4s, Cu 4p, and Sb 5s, whereas the bands above the Fermi level are mostly Ba 5d, Ba 6s, Cu 4s, Cu 4p, Sb 5s, and Sb 5p. The PDOS of Cu shows that the energy level of Cu 3d is almost below the Fermi level and the 4s orbitals are located above the Fermi level; therefore, it would be reasonable to assign the copper atom as Cu^+. While the Ba atom, whose contribution below the Fermi level is very small, had lost the outmost electrons almost entirely, it would be assigned as Ba^{2+}. Thus, the charge balance in the title compound would be achieved as $(Ba^{2+})_2(Cu^+)_{14.63}(Sb)_{10}{}^{1.863-}$ assuming the average oxidation state of −1.863 for the Sb atom. Considering the apparent contribution of Sb 5p orbitals to the conduction band, the assumption that the Sb atom is not fully reduced to be Sb^{3-} is rational.

To estimate the stability of $Ba_2Cu_{15}Sb_{10}$, two more models were designed as $Ba_2Cu_{12}Sb_{10}$ and $Ba_2Cu_{18}Sb_{10}$ with the Cu2 site empty or fully occupied, respectively. The formation energy is defined as the total energy difference between the ternary compound and the sum of the corresponding constituent elements, as eq 1 indicates:

$$E_f(Ba_2Cu_xSb_{10}) = E_{Ba_2Cu_xSb_{10}} - 2E_{Ba} - xE_{Cu} - 10E_{Sb} \quad (1)$$

The formation energies of three compositions, $Ba_2(Cu1)_{12}Sb_{10}$, $Ba_2(Cu1)_{12}(Cu2)_3Sb_{10}$, and $Ba_2(Cu1)_{12}(Cu2)_6Sb_{10}$, are −470.17, −479.96, and −16.08 KJ/mol, respectively (Table 4). These results suggest that the least

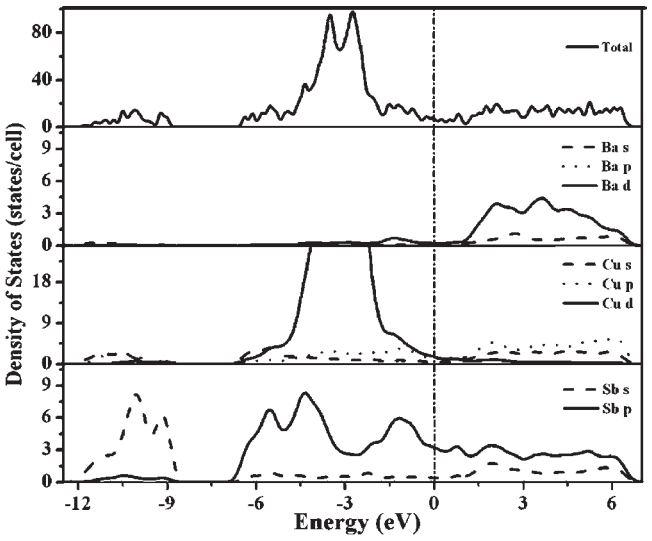

Figure 6. Total and partial densities of state for the hypothetical model of "$Ba_2Cu_{15}Sb_{10}$". (The Fermi level is set at 0 eV.)

Table 4. Calculated Formation Energies for $Ba_2Cu_xSb_{10}$ (x = 12, 15, 18)

model	total energy (eV p.u.c.)[a]	formation energy (eV p.u.c.)[a]	formation energy (KJ/mol)
$Ba_2(Cu1)_{12}Sb_{10}$	−19075.1178	−4.873	−470.17
$Ba_2(Cu1)_{12}(Cu2)_3Sb_{10}$	−23115.4147	−4.9745	−479.96
$Ba_2(Cu1)_{11}(Cu2)_4Sb_{10}$	−23112.9536	−2.5134	−242.51
$Ba_2(Cu1)_{12}(Cu2)_6Sb_{10}$	−27150.8023	−0.1667	−16.08

[a] eV per unit cell.

stable composition of them is $Ba_2(Cu1)_{12}(Cu2)_6Sb_{10}$ (with the Cu2 site fully occupied), which is over 450 KJ/mol higher in energy than the other two. And the formation energies of $Ba_2(Cu1)_{12}Sb_{10}$ (with empty Cu2 site) and $Ba_2(Cu1)_{12}(Cu2)_3Sb_{10}$ (with Cu2 site half occupied) are nearly the same, but $Ba_2(Cu1)_{12}(Cu2)_3Sb_{10}$ with the Cu2 site half occupied is 9.79 KJ/mol lower in energy and is the most stable one. Therefore, for the $BaNi_9P_5$-type Sb analogue, the Cu ~50% deficiency on the Cu2 site (6*h*) is energetically favorable. In comparison with the model $Ba_2(Cu1)_{12}(Cu2)_3Sb_{10}$ with three vacancies on the Cu2 site, we have also considered another situation, under which one of the three vacancies locates at Cu1 sites instead, namely, $Ba_2(Cu1)_{11}(Cu2)_4Sb_{10}$, whose formation energy is calculated to be −242.51 KJ/mol, higher than that of the model $Ba_2(Cu1)_{12}(Cu2)_3Sb_{10}$. Therefore, the vacancy at Cu1 sites is disfavored with respect to that at Cu2 sites in the structure. These support the single crystal refinement results described above.

Conclusion

A new Cu-rich caged antimonide, $BaCu_{7.31(3)}Sb_5$, has been synthesized and structurally characterized as the first antimony member of the $BaNi_9P_5$-type barium copper pnictides. The structure can be described in a clear way that the building unit, 30-vertex cage of $Cu_{18}Sb_{12}$ centered by a Ba atom, forms chains along the *c* axis by sharing opposite hexagonal Cu_3Sb_3 faces, and each chain fuses with six neighboring identical cage chains along the [100], [010], and [110] directions to generate a condensed 3D network. The electronic structure calculations by CASTEP suggest a metallic behavior, which agrees well with the electrical conductivity, Seebeck coefficient, and Pauli paramagnetic measurements. The Cu2 site deficiency turns out to be energetically favorable since the calculated formation energies indicate that $Ba_2Cu_{15}Sb_{10}$ (with a Cu2 site occupancy of 50%) is the most energetically favorable stoichiometry compared with $Ba_2Cu_{12}Sb_{10}$ (with an empty Cu2 site occupancy) and $Ba_2Cu_{18}Sb_{10}$ (with a Cu2 site occupancy of 100%), and a vacancy at the Cu1 site is disfavored in the structure. Due to the metallic nature of $BaCu_{7.31(3)}Sb_5$, this compound is not a good thermoelectric compound. However, its novel structure may shed useful light on the design of a new caged structure that is desired as a possible thermoelectric candidate.

Acknowledgment. This research was supported by the National Natural Science Foundation of China under Projects 90922021, 20773130, 20733003, 20821061, and 20973175; the "Knowledge Innovation Program of the Chinese Academy of Sciences" (KJCX2-YW-H20); and the "Key Project from CAS" (KJCX2-YW-H01).

Supporting Information Available: X-ray crystallographic files in CIF format. This material is available free of charge via the Internet at http://pubs.acs.org.